

Open access • Posted Content • DOI:10.1101/2020.01.07.897348

Computed tomography reveals hip dysplasia in Smilodon: Implications for social behavior in an extinct Pleistocene predator — Source link

Mairin Balisi, Abhinav K Sharma, Carrie M. Howard, Christopher A. Shaw ...+2 more authors

Institutions: Natural History Museum of Los Angeles County, University of California, Los Angeles, Idaho State University,

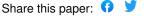
Cedars-Sinai Medical Center

Published on: 07 Jan 2020 - bioRxiv (Cold Spring Harbor Laboratory)

Topics: Smilodon

Related papers:

- · Computed tomography reveals hip dysplasia in the extinct Pleistocene saber-tooth cat Smilodon
- · Paleopathology in a nearly complete skeleton of Majungasaurus crenatissimus (Theropoda: Abelisauridae)
- · Hibernation in hominins from Atapuerca, Spain half a million years ago









Computed tomography reveals hip dysplasia in *Smilodon*:
Implications for social behavior in an extinct Pleistocene predator

- 6 Mairin A. Balisi^{1,2*}, Abhinav K. Sharma³, Carrie M. Howard¹, Christopher A.
- 7 Shaw^{1,4}, Robert Klapper⁵, Emily L. Lindsey¹
- 9 ¹ La Brea Tar Pits and Museum, Natural History Museum of Los Angeles County,
- 10 Los Angeles, California, United States of America
- 11 ² School of Natural Sciences, University of California, Merced, California, United
- 12 States of America

1

2

3

4 5

8

19

22

23

24

- 13 ³ David Geffen School of Medicine, University of California, Los Angeles,
- 14 California, United States of America
- ⁴ Idaho Museum of Natural History, Idaho State University, Pocatello, Idaho, United
- 16 States of America
- 17 ⁵ Orthopaedics, Cedars Sinai Medical Group, Los Angeles, California, United
- 18 States of America
- 20 * Corresponding author
- 21 E-mail: mbalisi@tarpits.org

Abstract

25

26

27

28

29

30

31

32

33

34

35

36

37

38

39

40

41

42

43

44

45

46

47

Reconstructing the behavior of extinct species is challenging, particularly for those with no living analogues. However, damage preserved as paleopathologies on bone can record how an animal moved in life, potentially reflecting patterns of behavior. Here, for the first time, we use computed tomography (CT) to assess hypothesized etiologies of pathology in a pelvis and associated right femur of an adult *Smilodon* fatalis saber-toothed cat, one of the best-studied mammal species from the Pleistoceneage Rancho La Brea asphalt seeps, Los Angeles, California. The pelvis exhibits massive destruction of the right acetabulum that previously was interpreted, for nearly a century, to have resulted from trauma and infection. We evaluated this historical interpretation using CT imaging to supplement gross morphology in identifying symptoms of traumatic, infective, or degenerative arthritis. We found that the pathologic distortions are inconsistent with degenerative changes that started only later in life, as in the case of infective or traumatic arthritis. Rather, they characterize chronic remodeling that began at birth and led to degeneration of the joint over time. These findings suggest that this individual suffered from hip dysplasia, a congenital condition common in domestic dogs and cats. The individual examined in this study reached adulthood (at least four to seven years of age) but never could have hunted properly nor defended territory on its own. As such, this individual, and other critically pathologic Smilodon like it, likely survived to adulthood by association with a social group that assisted it with feeding and protection. The pathologic specimens examined here in detail are consistent with a spectrum of social strategies in *Smilodon* supported by a predominance of previous studies. This

application of a relatively new and interdisciplinary technique to an old question therefore informs the longstanding debate between social and solitary hypotheses for the behavior of an extinct predator.

Introduction

48

49

50

51

52

53

54

55

56

57

58

59

60

61

62

63

64

65

66

67

68

69

The saber-toothed cat Smilodon fatalis is one of the most well-studied apex predators from the late Pleistocene epoch, if not across the entire history of fossil mammals [1]. Much of our knowledge about this species comes from the Rancho La Brea asphalt seeps in Los Angeles, California, United States, which selectively trapped and preserved thousands of individuals of Smilodon from at least 50,000 years ago until the species' extinction approximately 11,000 years ago [1]. The seeps functioned as a carnivore trap: a large herbivore stuck in the asphalt inadvertently would attract large carnivores and scavengers, which themselves would become entrapped in great numbers [2]. Studies of Smilodon at Rancho La Brea have enabled reconstruction of its feeding behavior as an ambush predator specializing on herbivorous megafauna, inferences derived using independent approaches ranging from comparative morphology (e.g. [3]) to stable isotopes (e.g. [4]). As well, the abundant specimens include numerous examples of healed injuries, or pathologies [5]. Paleopathologies preserved as skeletal lesions are a phenomenon that tends to be rare at more typical fossil sites that do not involve preservation in asphalt, do not exhibit a carnivore bias, or generally have undergone different taphonomic processes; but this phenomenon is captured by Rancho La Brea's large sample sizes.

71

72

73

74

75

76

77

78

79

80

81

82

83

84

85

86

87

88

89

90

91

92

As bone remodels throughout an animal's life in response to stress, strain, and injury [6–9], paleopathologies can preserve a record of realized behavior and supplement the picture of potential behavior presented by skeletal morphology. Differences in the distribution of pathologies throughout the skeleton, for example, distinguish *Smilodon* from a contemporaneous predator, the dire wolf *Canis dirus*, reflecting differences between the two species in hunting behavior and potential prey preference corroborated by independently gathered data (e.g. [4]). While injuries in dire wolves tended to be concentrated around its distal limbs, supporting the hypothesis that it was a pursuit predator, Smilodon's injuries tended to cluster around the midline of its body, supporting inferences that it ambushed and grappled with prey [5]. As the aggregate result of how an animal moved over the course of its life, pathologies present a relatively direct record of the animal's interactions with its prey, its environment, and even its conspecifics—including, potentially, intraspecific interactions such as agonistic behavior and sociality. Sociality, the degree to which individuals live with conspecifics in groups or societies [10], is difficult to infer in *Smilodon* given that it has no direct living analogues. Estimated to have weighed between 160 and 350 kg [3,11], Smilodon was at least the size of the Siberian tiger (Panthera tigris altaica), the largest extant felid: some estimates reach 369 to 469 kg, placing *Smilodon* in the range of the largest extant ursids [12,13]. No felid living today has *Smilodon*'s elongate, knife-like canines or stocky and powerful build. As well, Smilodon (of the extinct felid lineage Machairodontinae) is distantly related to extant large felids (Felinae), introducing further uncertainty. Based on its robust morphology (e.g. [14,15]) and on evidence from stable isotopes (e.g. [4]), it

94

95

96

97

98

99

100

101

102

103

104

105

106

107

108

109

110

111

112

113

114

115

likely stalked and ambushed its prey; therefore, it may have been similar to the African lion (Panthera leo), which has a similar hunting strategy and is social [16]. Yet sociality varies across mammalian species, including among members of a single genus; other extant pantherines like tigers (*Panthera tigris*) are solitary [17], complicating inferences of behavior based on ancestral reconstructions. Advocates of the solitary-cat hypothesis cite Smilodon's small relative brain size determined using endocranial casts [18] as evidence of solitary behavior, because sociality exerts high cognitive demands [19,20]. However, compared to ungulates and primates, carnivores have tended to decouple sociality and relative brain size, so that a smaller braincase does not necessitate a lack of sociality [21]. The gregarious-cat hypothesis has drawn support from the high ratios of *Smilodon* relative to prey at Rancho La Brea [14,22,23] (although detractors point out that some extant large cats aggregate at kills and carcasses despite otherwise being solitary [20]) and from comparisons between Rancho La Brea and playback experiments used to estimate carnivore abundance in Africa, which suggest that the densities of *Smilodon* at Rancho La Brea are more consistent with it having been social rather than solitary [24,25]. The lack of size sexual dimorphism in Smilodon relative to living or fossil lions has supported monogamy rather than polygynous breeding in Smilodon, if the saber-tooth did have a social structure [26], Most relevant to the current study, the existence of healed injuries in *Smilodon* also has been interpreted as evidence for social behavior, with the assumption that recovering from serious injury would be difficult if not impossible without cooperative sociality [27]. The current study centers on a *Smilodon* specimen (LACMHC 131) that has earned the distinction of being "the most strikingly pathological object in the collection of

117

118

119

120

121

122

123

124

125

126

127

128

129

130

131

132

133

134

135

136

137

138

Rancho La Brea fossils" [22]. The specimen is a right innominate bone exhibiting massive distortion and destruction of the hip socket (Figure 1). Moodie [22], restricted in 1930 to an inspection of the gross morphology, regarded this specimen as having been infected following violent trauma, possibly during an encounter with a conspecific, which also led to dislocation of the femur from the hip. Moodie found no pathologic bones potentially associated with the injured innominate; because of disarticulation by flowing asphalt over thousands of years, associated elements are rarely encountered at Rancho La Brea. However, after over half a century, Shermis [23] described a pathologic femur (LACMHC 6963; Figure 2) associated with another pathologic pelvis. Later, this femur was determined to be associated instead with the Moodie specimen [27], enabling examination of the effects of a single injury on associated skeletal elements using newer technology. Fig 1. Photographs of LACMHC 131, a pathologic pelvis belonging to *Smilodon* fatalis. (A) Lateral view of right side showing destruction of the acetabulum: anterodorsal end to the right. (B) Lateral view of left side showing the intact acetabulum but exostoses around the anterodorsal acetabular rim; anterodorsal end to the left. (C) Dorsal and **(D)** ventral views showing asymmetry in the pelvis; anterior end to the right. Fig 2. Photographs of LACMHC 6963, a pathologic right femur belonging to Smilodon fatalis. (A) Anterior and (B) posterior views of full femur, excluding the distal epiphysis, which was broken after death; proximal end on the left. (C) Anterior and (D) posterior close-up views of the proximal end. (E) Dorsal close-up view of the femoral head, greater trochanter, and lesser trochanter in lower center background. (F) Lateral close-up view of the greater trochanter and lesser trochanter (lower center), which is

enlarged into a round knob. The upper scale bar refers to A and B and the lower scale bar refers to C, D, E, and F.

In the present study, we supplement gross morphology and analyze LACMHC 131 and 6963 using computed tomography, observing, for the first time, the internal bone structure of a pathologic non-primate mammal. We evaluate the historical inference that the injury was the result of trauma and assess different etiologies of pathology: traumatic arthritis, infective arthritis, or degenerative arthritis. Finally, we explore the implications of the diagnosis on reconstructions of sociality in *Smilodon* and the potential contribution of paleopathology to a growing interdisciplinary body of literature supporting sociality in this extinct predator.

Materials and Methods

All specimens examined are from the collections of the La Brea Tar Pits and Museum, part of the Los Angeles County Natural History Museum (LACM), Los Angeles, California. Different fossiliferous asphaltic deposits (which became manmade "pits" during the historical excavation process) at Rancho La Brea had different periods of asphalt seep activity, thus entrapping organisms over different timespans over the past 55,000 years with varied depositional environments and taphonomic histories. In this context, we reduced potential variability in these factors by selecting all specimens from a single deposit, Pit 61/67. Pit 61/67 is the most recent deposit at Rancho La Brea that precedes the late Pleistocene megafaunal extinctions at around 11,000 years before present [28], at which point *Smilodon fatalis* became extinct.

162

163

164

165

166

167

168

169

170

171

172

173

174

175

176

177

178

179

180

We examined the external surfaces of the pathologic pelvis including the right innominate (LACMHC 131) and associated pathologic right femur (LACMHC 6963). As specimens for comparison, we inspected an unassociated non-pathologic right femur (LACMHC K-3232) and a non-pathologic pelvis (LACMHC K-2584) from the same deposit and of similar sizes and ontogenetic stages as the pathologic specimens. Initial surface scanning of all specimens was carried out using an Artec Space Spider (Artec 3D) as a means of digital preservation and to provide a 3D visual with color. The surface scans were processed in Artec Studio 12 and fused into a model with a resolution of 0.2 mm. CT imaging of LACMHC 131, 6963, and K-3232 was performed at the S. Mark Taper Foundation Imaging Center, Los Angeles, California, on a GE Revolution (GE Healthcare, Waukesha, WI) 256-slice scanner with 0.625 mm slice thickness. Imaging parameters were KVP=120, mA=300, 0.5 second rotation time, and 0.51 pitch using a medium body FOV. The data were acquired in the axial plane, reformatted into soft tissue and bone algorithms, and viewed in the axial, coronal and sagittal planes. CT images were converted to 3D models using the segmentation software Mimics (Materialise). Geomagic Freeform (3D Systems) was used to upload and determine placement of the plane for cross-sections of the 3D reconstructions. No permits were required for the described study, which complied with all relevant regulations.

Results

181

182

183

184

185

186

187

188

189

190

191

192

193

194

195

196

197

198

199

200

201

202

203

LACMHC 131 is a pathologic but complete pelvis with all sutures completely fused (Figure 1; File S1; Movie S1). The distal end of LACMHC 6963, the pathologic femur, is broken and missing (Figure 2; File S1), precluding verification of distal epiphyseal fusion. However, the proximal epiphyses are completely fused to the shaft, and the size of the femur is comparable to large adult femora belonging to other *Smilodon* preserved at Rancho La Brea. Therefore, the *Smilodon* individual represented by these two specimens is inferred to have been of adult age.

There are no signs of callus, or bone regeneration and healing, that typically are seen on imaging following fracture. Rather, the osteophytes are likely a sign of bone remodeling secondary to malformation of the joint with subsequent necrosis. The changes in the right acetabulum and right femur are consistent with those expected from repetitive subluxation and subsequent necrosis. The right acetabulum is shallow and elliptical-shaped as opposed to concentric-shaped. A hole in the bone, likely the result of posthumous asphaltic wear based on its sharp edges, marks the thin medial wall of the acetabulum, which is lined otherwise with exostoses. The left acetabulum appears non-pathologic; however, the ilium anterodorsal to the acetabulum—origin of the quadriceps femoris muscles—bears rugose ridges (Figure 1; File S1, Movie S1) absent on typical *Smilodon* pelvic specimens (Figure 3). The head of the pathologic right femur is flattened and laden with anatomical distortions; as well, the lesser trochanter is enlarged into a round knob (Figure 2; File S1). The non-pathologic right femur, the comparative specimen, bears a round head that is appropriately developed (Figure 4), fitting snugly into a concentric-shaped socket such as the left acetabulum of

205

206

207

208

209

210

211

212

213

214

215

216

217

218

219

220

221

222

223

224

225

226

the pathologic pelvis or either acetabulum of the non-pathologic pelvis (Figure 3) and thereby allowing for an axis of rotation and movement expected for *Smilodon* to function normally. Fig 3. Photographs of LACMHC K-2584, a non-pathologic pelvis belonging to Smilodon fatalis. (A) Lateral view of right side; anterodorsal end to the right. (B) Lateral view of left side; anterodorsal end to the left. (C) Dorsal and (D) ventral views; anterior end to the right. Fig 4. Photographs of LACMHC K-3232, a non-pathologic right femur belonging to Smilodon fatalis. (A) Anterior and (B) posterior views of full femur; proximal end on the left. (C) Anterior and (D) posterior close-up views of the proximal end, including the spherical femoral head, greater trochanter, and lesser trochanter. (E) Dorsal close-up view of the femoral head, greater trochanter, and lesser trochanter in lower center background. (F) Lateral close-up view of the greater trochanter and lesser trochanter (lower center). The upper scale bar refers to A and B and the lower scale bar refers to C, D, E, and F. The four cardinal findings of arthritis on imaging are bony sclerosis, osteophytes. joint space narrowing, and subchondral cysts. The CT images of the pathologic specimens reveal evidence of degenerative changes in the right hip joint and a lack of fractures from traumatic impact (Movie S2; Datasets S1-S3). The images demonstrate findings of sclerosis and osteophytes in both the right acetabulum and femoral head. which are changes consistent with degenerative arthritis. Profuse remodeling with osteophyte formation marks the right femoral head, likely in response to the

degenerative process from repeated subluxation and dysplasia.

Discussion

Diagnosis

The arthritic degeneration seen in the pathologic specimens and visualized on CT imaging must have arisen from one of three etiologies: traumatic arthritis, infective arthritis, or degenerative arthritis. Findings on the specimens make the etiologies of infective arthritis or traumatic arthritis less likely. In the case of infective arthritis, the presupposition is that the specimen developed typically before an insult that led to infection and subsequent obliteration of the hip joint. This assumption also holds true for the case of a traumatic arthritis etiology following an injury or fracture.

However, the anatomical distortions of the right femoral head, in conjunction with the obliteration of the right acetabulum seen in the gross specimens as well as on CT imaging, suggest chronic changes that led to degeneration over time (Figure 2). The degeneration of the head of the femur as seen would not be expected if the etiology of degenerative change in the hip joint were due to infection or trauma, as the development of the pelvis and femur presumably would have been complete before the insult or injury occurred during the adult cat's life.

Instead, the condition of the right acetabulum and right femoral head demonstrates anatomy consistent with developmental distortion. Typically, the head of the femur develops in conjunction with the acetabulum of the pelvis [29]. The spherical femoral head fits into the concentric-shaped acetabulum to form a ball-and-socket joint that enables a four-legged creature to ambulate normally, lie down, sit down, stand up,

and function without subluxation, or displacement, of the femoral head out of the pelvic socket [29]. In developmental hip dysplasia, however, the acetabulum of the pelvis does not develop appropriately, which subsequently affects the development of the head of the femur [29]. An elliptical acetabulum, as opposed to concentric-shaped, causes continual subluxation of the femoral head, which can result in coxa plana, or necrosis of the bony nucleus of the femoral head. This subsequent coxa plana produces flattening and degeneration of the normally spherical femoral head [30].

Proper anatomical development and ossification of the hip joint rely on continuous and symmetrical pressure of the femoral head on the acetabulum, and dysplasia results from improper positioning of the femoral head within the acetabulum [29,31]. Dysplastic hips are characterized by a pathologic restructuring of the hip and accelerated remodeling of the joint in response to abnormal forces and tensions that create stress. This produces formation of new bone in some areas and resorption of bone in others, ultimately causing degenerative joint disease [29].

This pathology starts to impact movement at the time of first walking, although minimal pain would ensue because of the animal's flexibility at its early age. As the joint cartilage wears out, however, bone would rub on bone. The ensuing forces would make the bone stiffer, resulting in osteophytes or bone spurs as well as sclerosis that manifests on CT imaging as increased bone density (Movie S2; Datasets S1-S2). At this point, loading the limb would cause pain, and range of motion would be limited. Therefore, the animal examined in this study would have spent as little time as possible on its right hind leg, needing to compensate for the handicap by increasing the load on its left hind leg. This compensation would explain the exostoses on the left ilium

anterodorsal to the otherwise non-pathologic acetabulum (Figure 1; File S1; Movie S1), indicating abnormal pulling of the quadriceps femoris muscles originating in this area.

Hip dysplasia in modern carnivorans

Hip dysplasia is a heritable, polygenic condition that can affect a range of mammal species [29], including humans [32–34]. Feline hip dysplasia is reported clinically relatively rarely [35,36], but canine hip dysplasia (CHD) is one of the most prevalent orthopedic diseases in domestic dogs [37] and, since it is similar to developmental dysplasia of the human hip [38], is very well studied.

Embryologically, articular joints differentiate from skeletal mesenchyme *in situ* with the support of surrounding tissues that sustain mechanical and physiological forces that tend to pull on the joints [29,39]. Dog hip joints are normal at birth, as teratologic factors and the mechanical stresses that could displace the femoral head are rare at this time [29]. In humans, fetus positioning—particularly the legs in adduction and extension—contributes to the development of hip dysplasia; the congruity of the acetabulum and femoral head is not maintained, making joint laxity more likely [29]. Additionally, suboptimal muscle function may be a major contributor to joint laxity, which in turn has been postulated to be a major contributor to the characteristic acetabular and femoral changes observed in hip dysplasia [29].

Epiphyseal ossification normally begins by 12 days of age in canines. In canines that eventually develop CHD, anatomical changes of the femoral head and pelvic socket begin prior to week three of development [40]. In dysplastic hips, the teres ligament, which is crucial for holding the femoral head in place, is too short; this produces luxation, or dislocation, of the top of the femoral head, beginning at around seven weeks

of age [29]. This luxation increases throughout development, degrading the articular cartilage that surrounds the femoral head and delaying ossification of the femur and acetabulum [29]. Dysplasia also results in shortening of the affected limb, as the femoral head is positioned higher in the acetabulum.

The overall results of these physiologic changes are mechanical imbalance and instability in the hip joint causing displacement due to opposing forces from the acetabulum and femoral head, and osteophytes in the acetabulum to compensate for cartilage loss [29].

Hip dysplasia and osteoarthritis in domestic and wild cats

Feline hip dysplasia (FHD) often is not detected clinically in domestic cats [36,41], possibly because it does not commonly cause overt functional impairment or because cats are able to compensate for the resulting lameness better than dogs [42,43]. As a result, much fewer clinical cases of FHD are reported [35,36] in contrast to cases of CHD [37]. In these cases, osteoarthritis (also known as degenerative joint disease, or DJD) of the hip secondary to FHD is well known [44]. Osteoarthritis was recorded in 43 of 45 (95.6%) of cats with FHD [45]. As well, in 5 of 13 (38.5%) cases of hip osteoarthritis with an identifiable radiographic or historical cause, hip dysplasia was pinpointed as the cause, with the remaining cases resulting from trauma or equivocal between trauma and dysplasia [42].

Reports of FHD in non-domestic large cats are even rarer than in domestic cats. Snow leopards in zoologic institutions have exhibited hip dysplasia; across 14 zoos, seven cases were classified as moderate to severe [46,47]. At least two individual snow leopards necessitated total hip replacement before being able to breed [46,47]. Beyond

snow leopards, accounts of functional impairment in the hip of non-domestic large cats tend to report osteoarthritis, which can be associated with FHD but may also stem from trauma and increased age [48–50].

For wild-caught large cats, the only comprehensive study of which we are aware is a survey of 386 individuals (283 wild-caught) across three felid genera mounted as exhibit skeletons in a range of North American natural history museums [49]. Though not focusing specifically on hip dysplasia, the study tracked DJD, which may be associated with hip dysplasia [42,45]. The sample recorded DJD in 9.7% of 31 tigers, 2.3% of 88 African lions, and 5.1% of 59 mountain lions, and none in five other species of big cat. These frequencies are low compared to domestic cats, perhaps owing to differences in body size, diet, and lifestyle between large wild cats and domestic cats [44]. Though this study identified instances of non-inflammatory osteoarthritis in the shoulder, elbow, and stifle, it found none in the hip. However, 4% of all joints afflicted by spondyloarthropathy—a form of inflammatory arthritis—comprised the hip [49].

Behavioral implications for *Smilodon*

Previous workers have inferred social behavior from *Smilodon's* pathologies, interpreting signs of healing as evidence that the animal continued to live after injury. Given the severity of many of the injuries, authors argue, the animal would have starved to death had it not lived within a social structure. The fact that the present pathology would have manifested from a young age, hindering the animal's ability to hunt prey and defend territory over the course of its life, is even more indicative of social structure.

Smilodon's large body size necessitated preying on megaherbivores for adequate sustenance [3]. To do so, like most large cats today, they would have used

their hindlimbs for propulsion and acceleration [51–53]. This pounce behavior would have been emphasized in *Smilodon*. Its ratio of total forelimb length to total hindlimb length is greater than those of living felids, while its ratio of tibia length to femur length ranks lower than those of living felids [14]. The shorter hindlimbs lacking the distal limb elongation seen in cursorial animals suggest that *Smilodon* was an ambush predator surpassing the ability of felids today [54]. Hunting large prey is dangerous [55]; after the initial leap powered by its hindlimbs, *Smilodon* would have grappled with its struggling prey, as evidenced by traumatic injuries radiating dorsolaterally to where the ribs articulate with the spine [5]. As it subdued prey with its robust forelimbs [15,52] under enough torque to injure the lumbar vertebrae [5], *Smilodon* would have needed to leverage itself against the ground using its hindlimbs. Therefore, the pelvis and femur would have been critical to multiple phases of *Smilodon*'s hunting strategy.

The dysplastic individual would have encountered much difficulty hunting in this manner. Yet, as evidenced by its large size and by complete fusion of its pelvic and femoral elements, it had reached adult age. (Studies of the detailed timing of epiphyseal fusion in large wild cats are lacking, but distal femoral epiphyses fuse at around the same time as or soon after proximal femoral epiphyses in domestic cats and dogs [56,57]; given this, the broken distal end likely also had a fused epiphysis.) Adulthood in *Smilodon* is likely equivalent to at least four years old, given that the forelimb and/or hindlimb in the African lion completely fuses between 4.5 and 5.5 years of age [58–60]; this is supported by bone histological work quantifying at least four lines of arrested growth (LAGs; one per growth year) in limb bones with fused epiphyses belonging to *Smilodon fatalis* from the Talara asphaltic deposits in Peru [61]. Some of the LAGs in

the *Smilodon* histological specimens likely have been masked by secondary bone remodeling [61], which may be more extensive in larger-bodied taxa [62], and these specimens may be older than the number of visible LAGs suggest; therefore, the pathologic specimen may be quite a bit older than four years of age.

To sustain growth to this age, the animal must have secured prey items without necessarily hunting them. We propose that this individual, and other critically pathologic *Smilodon* like it, survived to adulthood by association with a social group that assisted it with feeding and protection. Evidence for sociality in *Smilodon* historically has been drawn from three main sources: quantification of sexual dimorphism in the size and shape of skeletal elements, ontogenetic patterns in teeth and bone, and comparisons of Rancho La Brea with extant carnivore communities comprising social and solitary members.

Extant large felids are predominantly solitary, with neighboring and often related females tending to feed cooperatively more often and in larger numbers than males. The pride-dwelling, male-dominated African lion is the social outlier, though African lion females aggregate as well [63]. High levels of sexual dimorphism mark the African lion: males have manes, larger body size, and upper canines 25% larger than in females [64,65]. Rancho La Brea *Smilodon fatalis* exhibits discernible levels of sexual dimorphism in its canine teeth but less pronounced than the African lion's, suggesting that its social structure differed from that of *P. leo* [26]. Instead, *Smilodon* may have been solitary with females occasionally sharing prey, as is the case for most extant felids with low craniodental sexual dimorphism; or—if social—then its breeding system likely differed from those of any large felids today [26].

In Rancho La Brea *Smilodon*, levels of sexual dimorphism in overall cranial shape (though not size) are on par with those in extant pantherine cats, supporting the existence of a social structure in *Smilodon* [66]. However, pantherines span the social African lion to the solitary leopard (*Panthera pardus*), and therefore this comparison generated equivocal support for solitary polygyny or unisexual groups [66]. On the other hand, sexual dimorphism in various craniodental measurements for *Smilodon fatalis* from Talara is greater than at RLB and more consistent with sociality; the higher proportion of females to males at Talara further supports cooperative hunting among females [61]. Among social carnivorans today, social structure varies by resource level: larger groups during times of plenty or in the presence of competitors; pairs or individuals when resources are limited [67,68]. The difference in *Smilodon* sexual dimorphism between Rancho La Brea and Talara may well reflect true differences in social structure stemming from differences in competitor density or resource limitation, which may vary across sites or through time.

Ontogenetic growth patterns in teeth and bone support inferences of sociality from skeletal sexual dimorphism. In *Smilodon*, the teeth appear to mature earlier than when sutures and long-bone epiphyses fuse. At Rancho La Brea, most sampled specimens show significant pulp cavity closure of the lower canine (14 of 19 specimens over approximately 80% closure), a sign of dental maturation [69]. In contrast, RLB pantherine pulp cavities compared against the *Smilodon* sample were more evenly distributed across the closure percentage range—suggesting that the asphalt seeps tended to trap older *Smilodon* or, more likely (because other assessments have yielded estimates of a full range of ages in *Smilodon* [70]), that teeth mature earlier in *Smilodon*

than in pantherines. At Talara, age determination by dentition yields low estimated counts of juveniles, but age determination based on limb epiphyseal fusion yields 41% juveniles [61]. Histology of Talara *Smilodon* long bones reinforces this mismatch, as an apparent adult femur with fused epiphyses and seven LAGs may have been still growing, based on the lack of avascular and acellular subperiosteal lamellar bone [61]. The lag in maturation between the teeth and the limb bones suggests delayed weaning, prolonged juvenile dependence, and extended familial care until the full adult hunting morphology—saber canines and robust limbs—was complete. This social scenario would help explain how the individual in this current study was able to survive to adulthood given its debilitating handicap.

Lastly, the relatively high abundance of *Smilodon fatalis*—the most abundant carnivoran at Rancho La Brea, second to the dire wolf—has been interpreted as evidence for sociality. A full range of ages is present among Rancho La Brea *Smilodon*; in contrast, animals interpreted to be solitary, such as the American lion *Panthera atrox*, are represented largely by adult individuals [70]. Furthermore, the proportions of social and solitary species at Rancho La Brea parallel those drawn to audio playbacks of herbivore distress calls in the African savanna [24,25]. Extant social felids occur in higher densities than solitary species, and multiple individuals congregate around fresh kills; therefore, the high incidence of *S. fatalis* at Rancho La Brea makes sense less if it were solitary and more so if it were social.

Conclusions

Novel application of computed tomography to an old question of paleopathology has enabled diagnosis of hip dysplasia, a lifelong condition, in an individual *Smilodon fatalis* saber-toothed cat, informing the longstanding debate between social and solitary hypotheses for the behavior of this extinct predator. This individual likely was not the only *Smilodon* afflicted with hip dysplasia and preserved by the asphalt seeps; at least one other pelvic specimen—described by Shermis [23]—appears superficially similar to the pelvis examined in this study, and further study may reveal it to be dysplastic as well. The individual examined in this study reached adulthood (at least four to seven years of age) but could never have hunted nor defended territory on its own, given its locomotor impairment that would have been present since infancy. As such, this individual likely survived to adulthood by association with a social group that assisted it with feeding and protection.

Further conclusions are limited by the lack of a comprehensive and systematic comparative dataset comprising pathologic postcranial specimens from extant species, a persistent limitation of paleopathological studies [5]. Natural history museums may acquire cranial remains from zoos or similar institutions but often lack storage to accommodate postcranial skeletons, especially for large carnivores. While radiographic studies on domestic cats and dogs are informative as to the nature of hip dysplasia, these studies tend to examine pathologic bones *in situ*, still embedded in a muscular framework, as opposed to the isolated context in which paleopathological specimens are found. Computed tomography may be key to building such a dataset in the future.

Within the scope of this study, we cannot completely rule out the hypothesis that the pathologic animal was a scavenger and therefore could have obtained food outside the context of a social structure. It is also possible that, despite its disability, its large body size and fearsome canines made it a strong interference competitor. However, the pathologic specimens that we have examined here in detail are consistent with the predominance of studies supporting a spectrum of social strategies in this extinct predator. In many extant carnivores, sociality offers the benefits of cooperative hunting and cooperative rearing of young [71]. These benefits likely also applied to the extinct *Smilodon* in the late Pleistocene. As *Smilodon* coexisted with a rich megafaunal carnivore assemblage including dire wolves, American lions, and short-faced bears, cooperative sociality may have aided its success as a predator in a crowded field.

Acknowledgements

We thank Aisling Farrell at La Brea Tar Pits and Museum for facilitating specimen loans; CT segmentation specialists at the S. Mark Taper Foundation Imaging Center for CT-scanning specimens; Jeff Busey and Jessica Butler at Zimmer Biomet for aiding design of 3D models; and Alexis Mychajliw, Karin Rice, and Blaire Van Valkenburgh for comments and constructive discussion.

References

Werdelin L, McDonald HG, Shaw CA, editors. Smilodon: The Iconic Sabertooth.
 Baltimore, MD: Johns Hopkins University Press; 2018.

2. 475 Spencer LM, Van Valkenburgh B, Harris JM. Taphonomic analysis of large 476 mammals recovered from the Pleistocene Rancho La Brea tar seeps. 477 Paleobiology. 2003;29: 561–575. 3. Van Valkenburgh B, Hayward MW, Ripple WJ, Meloro C, Roth VL. The impact of 478 large terrestrial carnivores on Pleistocene ecosystems. Proc Natl Acad Sci. 479 2016;113: 862-867. doi:10.1073/pnas.1502554112 480 DeSantis LRG, Crites JM, Feranec RS, Fox-Dobbs K, Farrell AB, Harris JM, et al. 481 4. 482 Causes and consequences of Pleistocene megafaunal extinctions as revealed 483 from Rancho La Brea mammals. Curr Biol. 2019;29: 2488-2495.e2. 484 doi:10.1016/j.cub.2019.06.059 485 5. Brown C, Balisi M, Shaw CA, Van Valkenburgh B. Skeletal trauma reflects hunting behaviour in extinct sabre-tooth cats and dire wolves. Nat Ecol Evol. 486 487 2017;1: 1-7. doi:10.1038/s41559-017-0131 488 6. Rubin CT. Skeletal strain and the functional significance of bone architecture. 489 Calcif Tissue Int. 1984;36: 11–18. doi:10.1007/BF02406128 490 7. Burr DB, Martin RB, Schaffler MB, Radin EL. Bone remodeling in response to in 491 vivo fatique microdamage. J Biomech. 1985;18: 189-200. doi:10.1016/0021-9290(85)90204-0 492 Martin RB. Fatigue damage, remodeling, and the minimization of skeletal weight. 493 8. J Theor Biol. 2003;220: 271–276. doi:10.1006/jtbi.2003.3148 494 495 9. Taylor D, Hazenberg JG, Lee TC. Living with cracks: Damage and repair in 496 human bone. Nat Mater. 2007;6: 263–268. doi:10.1038/nmat1866 497 10. Eisenberg JF. The social organisation of mammals. Handb der Zool. 1966;10: 1498 92. Christiansen P, Harris JM. Body size of Smilodon (Mammalia: Felidae). J 499 11. 500 Morphol. 2005;266: 369–384. doi:10.1002/jmor.10384 501 12. Anyonge W. Body mass in large extant and extinct carnivores. J Zool. 1993;231: 502 339–350. 503 13. Torregrosa V, Petrucci M, Pérez-Claros JA, Palmqvist P. Nasal aperture area and body mass in felids: Ecophysiological implications and paleobiological inferences. 504 505 Geobios. 2010;43: 653–661. doi:10.1016/j.geobios.2010.05.001 506 14. Gonyea WJ. Behavioral implications of saber-toothed felid morphology. 507 Paleobiology. 1976;2: 332–342. 508 15. Meachen-Samuels JA. Morphological convergence of the prey-killing arsenal of sabertooth predators. Paleobiology. 2012;38: 1–14. doi:10.5061/dryad.h58q6 509 510 16. Schaller GB. The Serengeti lion: a study of predator-prey relations. University of Chicago Press; 1972. 511 Karanth KU, Sunguist ME. Behavioural correlates of predation by tiger (Panthera 512 17. 513 tigris), leopard (Panthera pardus), and dhole in Nagarahole, India. J Zool London. 514 2000;250: 255–265. Radinsky LB. Evolution of the felid brain. Brain Behav Evol. 1975;11: 214–254. 515 18. doi:10.1159/000123635 516 517 19. McCall S, Naples V, Martin LD. Assessing behavior in extinct animals: Was 518 Smilodon social? Brain Behav Evol. 2003;61: 159-164. doi:10.1159/000069752 519 20. Kiffner C. Coincidence or evidence: was the sabretooth cat Smilodon social? Biol 520 Lett. 2009;5: 561–562. doi:10.2307/5647

521 21. Pérez-Barbería FJ, Shultz S, Dunbar RIM. Evidence for coevolution of sociality 522 and relative brain size in three orders of mammals. Evolution (N Y). 2007;61: 523 2811–2821. doi:10.1111/j.1558-5646.2007.00229.x 524 22. Moodie RL. Pleistocene luxations. Am J Surg. 1930;IX: 348–362. 23. Shermis S. Healed massive pelvic fracture in a Smilodon from Rancho La Brea, 525 526 California. Paleobios. 1983;1: 121–126. 527 Carbone C, Maddox T, Funston PJ, Mills MGL, Grether GF, Van Valkenburgh B. 24. 528 Parallels between playbacks and Pleistocene tar seeps suggest sociality in an extinct sabretooth cat, Smilodon. Biol Lett. 2009;5: 81–85. 529 530 doi:10.1098/rsbl.2008.0526 531 25. Van Valkenburgh B, Maddox T, Funston PJ, Mills MGL, Grether GF, Carbone C. 532 Sociality in Rancho La Brea Smilodon: arguments favour 'evidence' over 'coincidence.' Biol Lett. 2009;5: 563-564. doi:10.1098/rsbl.2009.0261 533 Van Valkenburgh B, Sacco T. Sexual dimorphism, social behavior, and 534 26. intrasexual competition in large Pleistocene carnivorans. J Vertebr Paleontol. 535 536 2002;22: 164-169. doi:10.1671/0272-4634(2002)022[0164:SDSBAI]2.0.CO;2 537 27. Shaw CA, Ware CS. Smilodon paleopathology: a summary of research at Rancho La Brea. In: Werdelin L, Mcdonald HG, Shaw CA, editors. Smilodon: The Iconic 538 Sabertooth. Baltimore: Johns Hopkins University Press; 2018. 539 540 28. Fuller BT, Harris JM, Farrell AB, Takeuchi GT, Southon JR. Sample preparation 541 for radiocarbon dating and isotopic analysis of bone from Rancho La Brea. Nat Hist Museum Los Angeles Ctv Sci Ser. 2015;42: 151–167. 542 543 Riser WH, Rhodes WH, Newton CD. Hip dysplasia. Textbook of Small Animal 29.

544 Orthopaedics. J.B. Lippincott Company; 1985. 545 30. Creel R. Congenital hip dysplasia. Iowa State Univ Vet. 1961;23: 32–33. 546 doi:10.1097/00006416-198705000-00011 547 31. Peterson C. Canine hip dysplasia: Pathogenesis, phenotypic scoring, and genetics. Duluth J Undergrad Biol. 2017;4: 19–27. Available: 548 549 https://pubs.lib.umn.edu/index.php/djub/article/view/33 550 Ortolani M. Congenital hip dysplasia in the light of early and very early diagnosis. 32. 551 Clin Orthop Relat Res. 1976; No.119: 6-10. doi:10.1097/00003086-197609000-00003 552 553 33. Graf R. Fundamentals of sonographic diagnosis of infant hip dysplasia. J Pediatr 554 Orthop. 1984;4: 735–740. doi:10.1097/01241398-198411000-00015 Weinstein SL. Natural history of congenital dislocation and dysplasia. Clin Orthop 555 34. Relat Res. 1987;225: 62-76. 556 557 35. Holt PE. Hip dysplasia in a cat. J Small Anim Pract. 1978;19: 273–276. 558 doi:10.1111/j.1748-5827.1978.tb05490.x 559 36. Patsikas MN, Papazoglou LG, Komninou A, Dessiris AK, Tsimopoulos G. Hip 560 dysplasia in the cat: A report of three cases. J Small Anim Pract. 1998;39: 290-294. doi:10.1111/j.1748-5827.1998.tb03653.x 561 Bartolomé N, Segarra S, Artieda M, Francino O, Sánchez E, Szczypiorska M, et 562 37. al. A genetic predictive model for canine hip dysplasia: integration of Genome 563 564 Wide Association Study (GWAS) and candidate gene approaches. PLoS One. 2015;10: 1-13. doi:10.1371/journal.pone.0122558 565 Zhou Z, Sheng X, Zhang Z, Zhao K, Zhu L, Guo G, et al. Differential genetic 566 38.

567 regulation of canine hip dysplasia and osteoarthritis. PLoS One. 2010;5. doi:10.1371/journal.pone.0013219 568 569 39. Bollet AJ. The biology of degenerative joint disease. In: Sokoloff L, editor. Arthritis 570 & Rheumatism. Chicago: University of Chicago Press; 1969. pp. 144–162. Kealy RD, Lawler DF, Ballam JM, Lust G, Biery DN, Smith GK, et al. Evaluation of 571 40. 572 the effect of limited food consumption on radiographic evidence of osteoarthritis in dogs. J Am Vet Med Assoc. 2000;217: 1678–1680. 573 574 doi:10.2460/javma.2000.217.1678 Clarke SP, Bennett D. Feline osteoarthritis: A prospective study of 28 cases. J 575 41. 576 Small Anim Pract. 2006;47: 439–445. doi:10.1111/j.1748-5827.2006.00143.x 577 42. Clarke SP, Mellor D, Clements DN, Gemmill T, Farrell M, Carmicheal S, et al. 578 Prevalence of radiographic signs of degenerative joint disease in a hospital population of cats. Vet Rec. 2005;157: 793-799. doi:10.1136/vr.157.25.793 579 43. 580 Perry K. Feline hip dysplasia: A challenge to recognise and treat. J Feline Med Surg. 2016;18: 203–218. doi:10.1177/1098612X16631227 581 582 44. Lascelles BDX. Feline degenerative joint disease. Vet Surg. 2010;39: 2–13. 583 doi:10.1111/j.1532-950X.2009.00597.x Keller GG, Reed AL, Lattimer JC, Corley EA. Hip dysplasia: A feline population 584 45. 585 study. Vet Radiol Ultrasound. 1999;40: 460–464. doi:10.1111/j.1740-586 8261.1999.tb00375.x 587 46. Wharton D, Mainka SA. Management and husbandry of the snow leopard Uncia uncia. Int Zoo Yearb. 1997;35: 139–147. doi:10.1111/j.1748-1090.1997.tb01203.x 588 47. Suedmeyer WK, Cook JL, Tomlinson JL, Crouch DT. Bilateral total hip

589

590 replacement in a snow leopard (Uncia uncia) with bilateral hip dysplasia. International Association for Aquatic Animal Medicine. 2000. 591 592 48. Whiteside DP, Remedios AM, Black SR, Finn-Bodner ST. Meloxicam and surgical 593 denervation of the coxofemoral joint for the treatment of degenerative osteoarthritis in a Bengal tiger (Panthera tigris tigris). J Zoo Wildl Med. 2006;37: 594 595 416-419. doi:10.1638/05-078.1 596 Rothschild BM, Rothschild C, Woods RJ. Inflammatory arthritis in large cats: An 49. 597 expanded spectrum of spondyloarthropathy. J Zoo Wildl Med. 2010;29: 279–284. Napier JE, Lund MS, Armstrong DL, McAloose D. A retrospective study of 598 50. 599 morbidity and mortality in the North American Amur leopard (Panthera pardus 600 orientalis) population in zoologic institutions from 1992 to 2014. J Zoo Wildl Med. 601 2018;49: 70-78. doi:10.1638/2017-0019r2.1 Harris MA, Steudel K. Ecological correlates of hind-limb length in the Carnivora. 602 51. Journal of Zoology. 1997. pp. 381-408. doi:10.1111/j.1469-7998.1997.tb01966.x 603 604 52. Meachen-Samuels JA, van Valkenburgh B. Radiographs reveal exceptional 605 forelimb strength in the sabertooth cat, Smilodon fatalis. PLoS One. 2010;5. 606 doi:10.1371/journal.pone.0011412 Martín-Serra A, Figueirido B, Palmqvist P. A three-dimensional analysis of the 607 53. morphological evolution and locomotor behaviour of the carnivoran hind limb. 608 BMC Evol Biol. 2014;14: 1–13. doi:10.1186/1471-2148-14-129 609 610 54. Anyonge W. Locomotor behaviour in Plio-Pleistocene sabre-tooth cats: a biomechanical analysis. J Zool. 1996;238: 395-413. 611 612 Carbone C, Teacher A, Rowcliffe JM. The costs of carnivory. PLoS Biol. 2007;5: 55.

613 363–368. doi:10.1371/journal.pbio.0050022 614 56. Sumner-Smith G. Observations on epiphyseal fusion of the canine appendicular 615 skeleton. J Small Anim Pract. 1966;7: 303–311. doi:10.1111/j.1748-616 5827.1966.tb04447.x 617 Smith RN. Fusion of ossification centres in the cat. J Small Anim Pract. 1969;10: 57. 523–530. doi:10.1111/j.1748-5827.1969.tb04071.x 618 Smuts GL, Robinson GA, Whyte IJ. Comparative growth of wild male and female 619 58. 620 lions (Panthera leo). J Zool. 1980;190: 365-373. doi:10.1111/j.1469-7998.1980.tb01433.x 621 622 59. Kirberger RM, du Plessis WM, Turner PH. Radiologic anatomy of the normal 623 appendicular skeleton of the lion (Panthera leo). Part 1: thoracic limb. J Zoo Wildl 624 Med. 2005;36: 29–35. doi:10.1638/03-013 Kirberger RM, du Plessis WM, Turner PH. Radiologic anatomy of the normal 625 60. 626 appendicular skeleton of the lion (Panthera leo). Part 2: pelvic limb. J Zoo Wildl 627 Med. 2005;36: 29–35. doi:10.1638/03-013 628 61. Seymour KL, Reynolds AR, Churcher CS. Smilodon fatalis from Talara, Peru: 629 Sex, age, mass, and histology. In: Werdelin L, McDonald HG, Shaw C, editors. 630 Smilodon: The Iconic Sabertooth. Baltimore, MD: Johns Hopkins University Press; 2018. 631 632 62. Straehl FR, Schever TM. Evolutionary patterns of bone histology and bone compactness in xenarthran mammal long bones. PLoS One. 2013;8: 1-19. 633 doi:10.1371/journal.pone.0069275 634 Kitchener A. The Natural History of the Wild Cats. Ithaca, NY: Cornell University 635 63.

636		Press; 1991.
637	64.	Smuts GL, Anderson JL, Austin JC. Age determination of the African lion
638		(Panthera leo). J Zool. 1978;185: 115-146. doi:10.1111/j.1469-
639		7998.1978.tb03317.x
640	65.	Gittleman JL, Van Valkenburgh B. Sexual dimorphism in the canines and skulls of
641		carnivores: effects of size, phylogeny, and behavioural ecology. J Zool. 1997;242:
642		97–117.
643	66.	Christiansen P, Harris JM. Variation in craniomandibular morphology and sexual
644		dimorphism in pantherines and the sabercat Smilodon fatalis. PLoS One. 2012;7.
645		doi:10.1371/journal.pone.0048352
646	67.	Gese EM, Rongstad OJ, Mytton WR. Relationship between coyote group size and
647		diet in southeastern Colorado. J Wildl Manage. 1988;52: 647-653.
648	68.	Arjo WM, Pletscher DH. Behavioral responses of coyotes to wolf recolonization in
649		northwestern Montana. Can J Zool. 1999;77: 1919–1927. doi:10.1139/z99-177
650	69.	Meachen-Samuels JA, Binder WJ. Sexual dimorphism and ontogenetic growth in
651		the American lion and sabertoothed cat from Rancho La Brea. J Zool. 2010;280:
652		271–279. doi:10.1111/j.1469-7998.2009.00659.x
653	70.	Miller GJ. On the distribution of Smilodon californicus Bovard from Rancho La
654		Brea. Los Angeles Cty Museum Contrib Sci. 1968;131: 1–19.
655	71.	Macdonald DW. The ecology of carnivore social behaviour. Nature. 1983;301:
656		379-384. doi:10.1016/0169-5347(89)90147-x
657		

Supporting Information

659

660

661

662

663

664

665

666

667

668

669

670

671

672

673

674

675

676

677

678

679

680

Movie S1. A video movie of a structured light surface scan of LACMHC 131, the pathologic pelvis belonging to Smilodon fatalis. Movie created in Adobe Photoshop CC by Carrie Howard. Movie S2. A video scrolling anteroposteriorly through LACMHC 131, the pathologic pelvis belonging to Smilodon fatalis. Ventral is at top. Video created by Carrie Howard from CT scans generated at the S. Mark Taper Foundation Imaging Center at Cedars Sinai Medical Group. File S1. Three-dimensional PDF of the pathologic pelvis (LACMHC 131) and femur (LACMHC 6963). Dataset S1. Compressed zip file containing the full computed tomography scan of LACMHC 131, the pathologic pelvis. Dataset S2. Compressed zip file containing the full computed tomography scan of LACMHC 6963, the pathologic femur. Dataset S3. Compressed zip file containing the full computed tomography scan of LACMHC K-3232, the non-pathologic right femur.

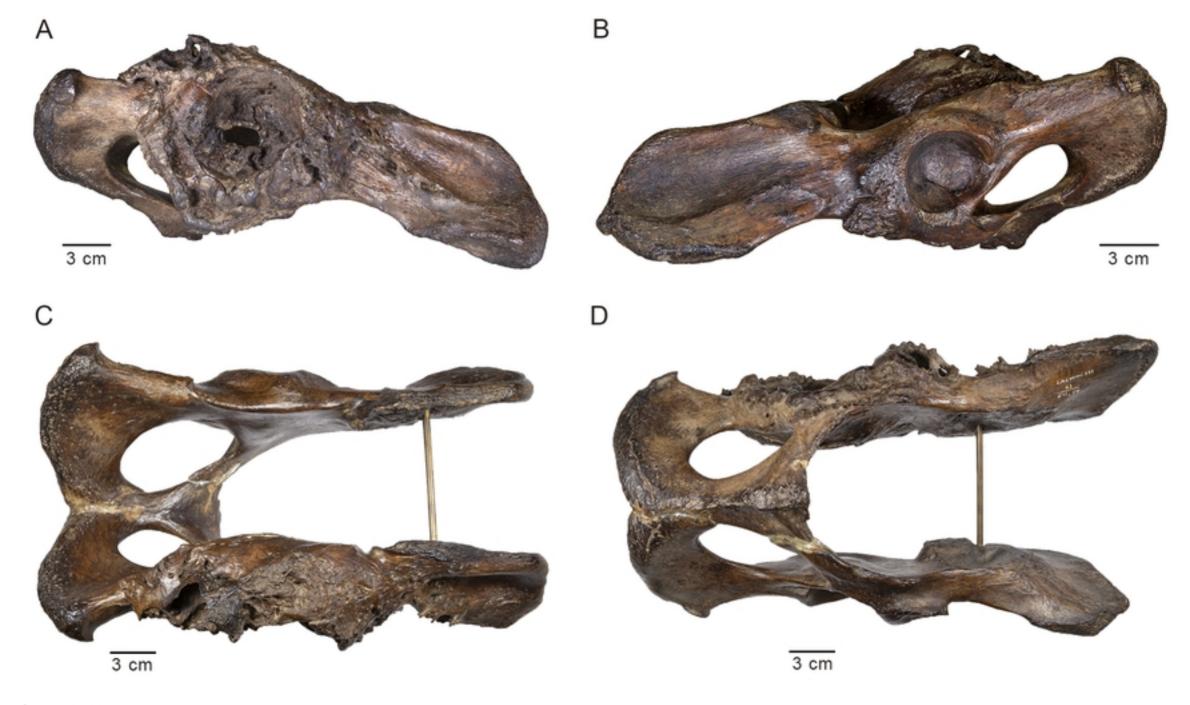


Figure 1

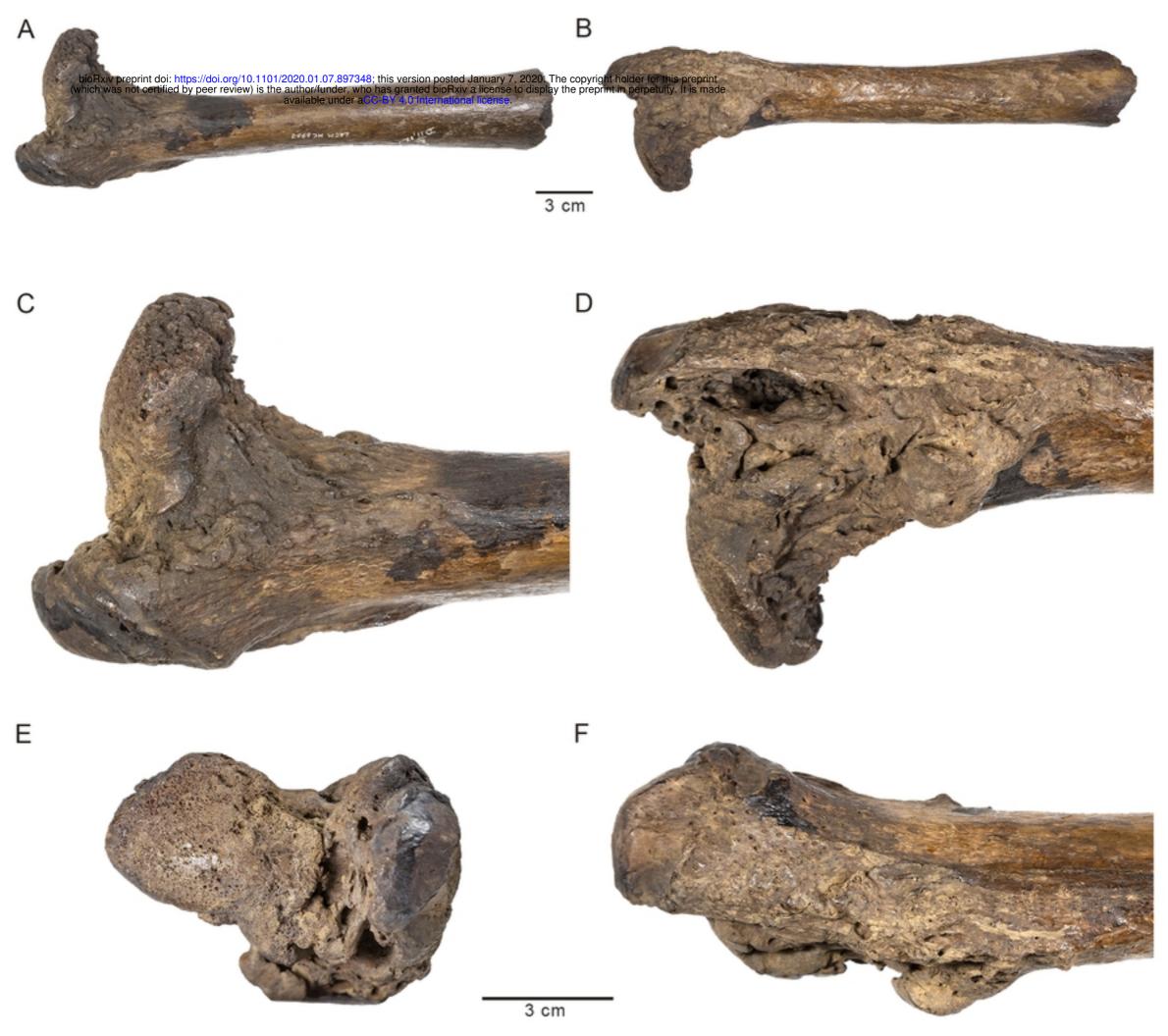


Figure 2



Figure 3



Figure 4